CrossMark

Voxel-based lesion-symptom mapping of stroke lesions underlying somatosensory deficits

Sarah Meyer[a],[*],[1], Simon S. Kessner[b],[1], Bastian Cheng[b], Marlene Bönstrup[b], Robert Schulz[b], Friedhelm C. Hummel[b], Nele De Bruyn[a], Andre Peeters[c], Vincent Van Pesch[c], Thierry Duprez[d], Stefan Sunaert[e],[f], Maarten Schrooten[g],[h], Hilde Feys[a], Christian Gerloff[b], Götz Thomalla[b], Vincent Thijs[g],[h],[i],[j], Geert Verheyden[a]

[a]KU Leuven — University of Leuven, Department of Rehabilitation Sciences, Tervuursevest 101/bus 1501, 3001 Leuven, Belgium
[b]University Medical Center Hamburg-Eppendorf, Department of Neurology, Martinistraße 52, 20246 Hamburg, Germany
[c]Cliniques Universitaires Saint-Luc, Department of Neurology, Hippokrateslaan 10, 1200 Brussels, Belgium
[d]Cliniques Universitaires Saint-Luc, Department of Radiology, Hippokrateslaan 10, 1200 Brussels, Belgium
[e]KU Leuven — University of Leuven, Department of Imaging and Pathology, Herestraat 49, 3000 Leuven, Belgium
[f]University Hospitals Leuven, Department of Radiology, Herestraat 49, 3000 Leuven, Belgium
[g]KU Leuven — University of Leuven, Department of Neurosciences, Herestraat 49, 3000 Leuven, Belgium
[h]University Hospitals Leuven, Department of Neurology, Herestraat 49, 3000 Leuven, Belgium
[i]Laboratory of Neurobiology, Vesalius Research Center, VIB, Herestraat 49, 3000 Leuven, Belgium
[j]KU Leuven — University of Leuven, Experimental Neurology and Leuven Research Institute for Neuroscience and Disease (LIND), Herestraat 49, 3000 Leuven, Belgium

ARTICLE INFO

ABSTRACT

The aim of this study was to investigate the relationship between stroke lesion location and the resulting somatosensory deficit. We studied exteroceptive and proprioceptive somatosensory symptoms and stroke lesions in 38 patients with first-ever acute stroke. The Erasmus modified Nottingham Sensory Assessment was used to clinically evaluate somatosensory functioning in the arm and hand within the first week after stroke onset. Additionally, more objective measures such as the perceptual threshold of touch and somatosensory evoked potentials were recorded. Non-parametric voxel-based lesion-symptom mapping was performed to investigate lesion contribution to different somatosensory deficits in the upper limb. Additionally, structural connectivity of brain areas that demonstrated the strongest association with somatosensory symptoms was determined, using probabilistic fiber tracking based on diffusion tensor imaging data from a healthy age-matched sample. Voxels with a significant association to somatosensory deficits were clustered in two core brain regions: the central parietal white matter, also referred to as the sensory component of the superior thalamic radiation, and the parietal operculum close to the insular cortex, representing the secondary somatosensory cortex. Our objective recordings confirmed findings from clinical assessments. Probabilistic tracking connected the first region to thalamus, internal capsule, brain stem, postcentral gyrus, cerebellum, and frontal pathways, while the second region demonstrated structural connections to thalamus, insular and primary somatosensory cortex. This study reveals that stroke lesions in the sensory fibers of the superior thalamocortical radiation and the parietal operculum are significantly associated with multiple exteroceptive and proprioceptive deficits in the arm and hand.

1. Introduction

Somatosensory deficits are common after stroke, with reported prevalence ranging from 11% to 85% (Connell et al., 2008; Tyson et al., 2008). While somatosensory symptoms after stroke may be discomforting and disabling by themselves, they further affect motor ability and overall rehabilitation after stroke. The somatosensory system

plays a crucial role in motor performance by providing constant sensory feedback to be able to make adaptations in an on-going motor task (Rabin and Gordon, 2004). As a consequence, somatosensory dysfunction represents an important factor for motor and functional outcome after stroke (Meyer et al., 2014; Tyson et al., 2008).

Somatosensation comprehends all anatomical components of the central and peripheral nervous systems that receive and interpret sensory information from receptors in the joints, ligaments, muscles, and skin. The somatosensory system has two primary functions: exteroceptive and proprioceptive sensation (DeJong, 1979). Exteroceptive sensation includes somatosensory modalities such as light touch, pressure, pinprick and pain (DeJong, 1979), whereas proprioceptive sensation is

the ability to recognize the location and movement of our limbs in space (Sherrington, 1907). Although somatosensory symptoms are present in a large number of stroke patients, detailed reports on the affected components of somatosensation are rare (Carey and Matyas, 2011; Connell et al., 2008; Tyson et al., 2008).

In contrast to the large amount of studies reporting on neural correlates of motor symptoms and recovery after stroke (Rehme et al., 2012; Ward et al., 2003), the relationship between lesion location and somatosensory deficits after stroke remains poorly understood. From primate studies, it is well-known that the ventral posterior lateral nucleus of the thalamus is an important brain structure in somatosensory processing, as both the dorsal and the anterolateral ascending tracts terminate in this nucleus (Martin and Jessel, 1991). Most somatosensory information enters the cerebral cortex through projections from the thalamus up to the primary somatosensory cortex (S1). Furthermore, small projections exist from the thalamus to the secondary somatosensory cortex (S2), the posterior parietal cortex and insular cortex (Burton and Jones, 1976). In humans, lesion studies using structural brain imaging revealed contributions of thalamus, lenticulocapsular region, corona radiata, and the brain stem to the occurrence of a somatosensory deficit (Georgiadis et al., 1999; Kim, 1992). With respect to the secondary somatosensory cortex in the human parietal operculum, several distinct cortical subdivisions were distinguished for either basic sensorimotor processing or higher order somatosensory processing (Eickhoff et al., 2010, Eickhoff et al., 2006b).

To the best of our knowledge, only two recent studies investigated the voxel-wise association between lesion location and a somatosensory deficit in patients after stroke (Baier et al., 2014; Preusser et al., 2014). It was found that impaired light touch perception was associated with lesions in S2, the anterior and posterior insular cortex, the putamen, and white matter connections reaching ventrally towards prefrontal brain areas (Dijkerman and de Haan, 2007; Preusser et al., 2014). The other voxel-wise association study, including patients with insular strokes, demonstrated that lesions in the posterior insular cortex are associated exclusively to impaired temperature perception (Baier et al., 2014). More detailed analysis of different somatosensory modalities has not been conducted as yet using modern voxel-based imaging methods. Thus, it remains unclear to what extent lesions in these brain areas affect other sensory modalities besides light touch and temperature perception. Therefore, the aim of the present study was to investigate, which brain regions are associated with the occurrence of different exteroceptive and proprioceptive somatosensory deficits in the acute phase after stroke, using voxel-based lesion-symptom mapping (VLSM).

2. Materials and methods

2.1. Patients

Thirty-eight consecutive adult patients were recruited for this study at the acute stroke unit of two University Hospitals in Belgium from October 2012 until September 2014. The inclusion criteria were (1) first-ever stroke (ischemic or hemorrhagic) as defined by the World Health Organization (World Health Organization MONICA Project, 1988); (2) assessment within the first week after stroke; (3) presence of motor and/or somatosensory deficit in the upper limb, using the Fugl–Meyer motor assessment upper extremity and somatosensory assessments as described below, and; (4) sufficient cooperation to perform the assessment. Patients were excluded if they (1) had a pre-stroke Barthel Index <95 out of 100; (2) had other serious neurological conditions with permanent damage; (3) had a subdural hematoma, tumor, encephalitis or trauma that led to similar symptoms as a stroke, and; (4) had serious communication, cognitive or language deficits, which could hamper the assessment. Patients signed a written informed consent form prior to participation. Ethical approval was obtained from the Ethics Committee of both University Hospitals in Leuven and Brussels.

2.2. Behavioral assessment

2.2.1. Testing procedure

Patients were assessed once within day 4 to day 7 after stroke onset using an MRI brain imaging protocol and clinical as well as more objective measures of somatosensory function. To ensure standardized data collection, the clinical testing was performed by only one trained physiotherapist (S.M.). Furthermore, patients' baseline characteristics were collected, and severity of stroke was assessed using the National Institutes of Health Stroke Scale (NIHSS). The presence of visuo-spatial neglect was assessed with the star cancellation test (Friedman, 1992), the most sensitive paper-and-pencil measure of visuo-spatial neglect (Lindell et al., 2007). A cut-off score of <44 (out of 54 stars) was used to determine the presence of visuo-spatial neglect.

2.2.2. Somatosensory assessment

Somatosensory deficits in the affected upper limb were assessed using the Erasmus MC modifications of the (revised) Nottingham sensory assessment, the perceptual threshold of touch (PTT), and somatosensory evoked potentials (SSEP).

The Erasmus MC modification of the (revised) Nottingham sensory assessment (Em-NSA) assesses light touch, pressure, pinprick and proprioception in the affected upper extremity and has good to excellent intra-rater and inter-rater reliability (Stolk-Hornsveld et al., 2006). Light touch was applied with a cotton wool, pressure with the index finger and pinprick with a toothpick, all at predefined points of contact. Proprioception was assessed during passive movements of the different joints in the upper limb. Scores for each modality range on a continuous scale from 0 (complete loss of somatosensory function) to 8 (intact somatosensory function). A cut-off score of <7 indicates the presence of somatosensory deficit.

The perceptual threshold of touch (PTT) is the minimal stimulus level of touch that is detectable. A transcutaneous electric nerve stimulation (TENS) was applied with a portable device, the CEFAR Primo Pro (Cefar Medical AB, Sweden). Round electrodes, with a diameter of 3 cm, were attached to the index finger and bulb of the thumb of the affected upper extremity. A high-frequency constant current of 40 Hz with single square pulses of 80 μs pulse duration was applied. The amplitude was gradually increased from 0 mA with increments of 0.5 mA, until a tingling sensation was perceived. To evaluate the PTT impairment, individual scores were compared to age- and gender-matched cut-off norm-values (Eek et al., 2012). Impairment was defined as a threshold value above the predefined norm value and therefore PTT scores were classified into impaired or normal PTT. Good reliability has been established for this method in stroke patients (Eek and Engardt, 2003).

Somatosensory evoked potentials (SSEP) were measured following a standardized protocol (American Clinical Neurophysiology Society, 2006). A transcutaneous electrical stimulation (monophasic rectangular pulses) was delivered to the median nerve at the wrist with a pulse of 200 μs and a stimulation rate of 5.1 Hz. The cathode was placed between the tendons of the palmaris longus and flexor carpi radialis muscles, the anode was placed 2 to 3 cm distal to the cathode and the ground electrode was placed on the forearm. Sensory threshold was determined on the non-affected side and stimulation was performed at 3 times this sensory threshold for both the unaffected and the affected side. Stimulation was always above motor threshold and produced a clearly visible muscle twitch causing abduction of the thumb. Standard 10 mm cup electrodes, connected to a Medelec Synergy System, were placed at positions CP3 and CP4, according to the international 10–5 system (Oostenveld and Praamstra, 2001). The SSEP assessment was consecutively performed at the non-affected and the affected upper limb. The interside difference between interpeak cortical amplitude N20-P25 was calculated. To evaluate the SSEP impairment, these

calculated scores were compared to norm-values of the interside difference of cortical amplitudes that were established in healthy persons with good reliability (Chiappa, 2003), and were then classified into impaired or normal.

2.3. Imaging

2.3.1. Data acquisition

Magnetic resonance images of the brain were obtained with a Philips 3T Achieve scanner. Either 3D or 2D fluid-attenuated inversion recovery imaging (FLAIR) data and diffusion-weighted images (DWI) were acquired at days 4 to 7 after stroke onset. Parameters settings for FLAIR sequences were: echo time = 350 ms, repetition time = 4800 ms, inversion time = 1650 ms, field of view = 250×250 mm^2, slice thickness = 1.12 mm, and gap = 0.56 mm. Parameter setting for DWI sequences were: echo time = 72 ms, repetition time = 12 s, b-value: 1300 s/mm^2, slice thickness = 2.5 mm, gap = 2.5 mm.

2.3.2. Lesion segmentation

As established in previous stroke imaging studies, individual stroke lesions of the patients were segmented on FLAIR sequences (Cheng et al., 2014). Therefore, we used an in-house developed software tool for the analysis of stroke imaging series (Antonia, Analysis Tool for Neuro Imaging Data) (Forkert et al., 2014). To this end, a rough region of interest (ROI) surrounding the hyperintense FLAIR lesion was drawn at each affected slice. In a subsequent step, a signal intensity threshold was manually applied to refine the final lesion segmentation. For hemorrhagic lesions, the perilesional edema was included into ROI, if restriction of diffusion was present. Accuracy of lesion delineation was inspected visually at each slice, and the corresponding diffusion-weighted images were consulted to confirm plausibility. All lesions were delineated by an experienced rater (S.S.K.). ROI from all slices were then concatenated to a volume of interest (VOI). FLAIR hyperintensities with no corresponding diffusion-restriction, representing leukoaraiosis or silent old stroke lesions (with no corresponding DWI lesion), were not included into the stroke lesion segmentation. Individual FLAIR datasets and lesion VOI were then registered to an in-house standard FLAIR brain template by linear transformation. This template has been previously created by normalization of FLAIR imaging data from 600 healthy volunteers in standard MNI (Montreal Neurological Institute) space (resolution of $2 \times 2 \times 2$ mm^3). The transformation parameters were then applied to the lesion VOI in order to ensure a standardized normalization for all individual stroke lesions.

2.3.3. Voxel-based lesion symptom mapping (VLSM)

Individual normalized FLAIR stroke lesions were entered into a voxel-based lesion-symptom mapping analysis using non-parametric mapping toolbox (NPM) from MRICron software package Version 6, 2013 (Rorden et al., 2007). In our sample, the right hemisphere was affected in 28 patients, the left hemisphere in 10 patients. To increase statistical power of identifying a lesion pattern with a significant contribution to somatosensory deficits independent of the lesioned hemisphere, all lesion maps were flipped onto the right hemisphere, as reported before (Cheng et al., 2014). First, a lesion overlap was calculated to create a color-coded overlay map of injured voxels across all patients to provide an overview of all lesioned brain areas. Second, the statistical contribution of lesion location to somatosensory deficit was tested using voxel-based lesion symptom mapping. Therefore, in each voxel a group comparison between patients having a lesion in this voxel and patients having no lesion in this voxel was estimated as Brunner–Munzel rank order using the clinical somatosensory scores of the four Em-NSA subscales with the full score range (i.e. light touch, pressure, pinprick and proprioception) as dependent variables resulting in four different statistical maps (Rorden et al., 2007). For appropriate Brunner–Munzel statistics, only voxels affected in at least 10 patients were tested (Medina et al., 2010). To correct for multiple comparisons,

all result maps were corrected using a threshold of 1% false discovery rate (FDR). In order to visualize the spatial distribution of brain voxels contributing to disturbance of the different somatosensory modalities, the four statistical maps from the somatosensory tests (light touch, pressure, pinprick and proprioception) were binarised at the threshold of significance (1% FDR) and overlaid. To describe key anatomical regions involved in somatosensory deficit, the peak voxel clusters were then identified from global maxima of the overlay map. These peak voxels were used as starting points for probabilistic fiber tracking (see below). Only for the PTT and the SSEP, dichotomous scores were entered into another VLSM analysis and Liebermeister statistics were estimated. For the PTT, a correction for multiple comparison was applied at a level of 1% FDR. For exploratory reasons, a more lenient threshold of 5% FDR was applied for results of SSEP, due to the higher rate of missing values of the SSEP variables.

2.3.4. Probabilistic fiber tracking

In healthy volunteers, we investigated connection probability of brain regions showing significant associations with somatosensory deficits using the probabilistic diffusion models and tractography implemented in the FSL software package 5.1 (http://www.fmrib.ox.ac.uk/fsl) (Behrens et al., 2007). To this end, we acquired diffusion weighted imaging data from 24 healthy, age-matched volunteers (mean age: 67 years, range: 32 to 78 years; unpaired t-test of age to current study sample of 38 patients: p = 0.4). A 3T Siemens Skyra MRI scanner (Siemens, Erlangen, Germany) and 32-channel head coil were used. 75 axial slices were obtained covering the whole brain with gradients (b = 1500 mm^2/s) applied along 64 non-collinear directions with the sequence parameters: Repetition time = 10,000 ms, echo time = 82 ms, field of view = 256×204, slice thickness = 2 mm, in-plane resolution = 2×2 mm^2. All datasets were corrected for eddy currents and head motion. Peak clusters resulting from Brunner–Munzel tests (x/y/z = 29/−25/25 and 35/−15/16) were used to generate a cubic cluster of 5×5 voxels using toolboxes provided by FSL. From each voxel, 10,000 samples were initiated through the probability fiber distribution of principle white matter fiber directions with a curvature threshold of 0.2. Resulting tract distributions were normalized in relation to the general connectivity profile in each individual volunteer. We applied a threshold of 100 samples (1% of 10,000 samples) following recommendations from the online documentation of the FSL library. Resulting tracts from all 24 volunteers were then registered to MNI space using the linear and non-linear transformation tools implemented in FSL (Jenkinson et al., 2012). A common tract was created using voxels that were found in at least 50% (12 of 24) of the participants. For anatomical comparisons, individual pyramidal tracts were additionally created analogously using the precentral cortex as seeding mask and waypoints in the posterior internal capsule and cerebral peduncle.

3. Results

We recruited 38 patients from two acute stroke units with a median of 6 days post stroke (range 4–7) (Table 1). The median age at stroke onset was 75 years (IQR 63–81) and 53% of the patients were males. The majority of the patients suffered from ischemic stroke (87%), whereas five patients presented with primary intracranial hemorrhage. A total of 28 patients (74%) had a lesion in the right hemisphere, and ten patients (26%) a lesion in the left hemisphere. Stroke severity was mild to severe with a score range on the NIHSS of 1 to 23, and a median score of 8.5 (IQR 6-13). Neglect was present in 8 patients (23%). A total of 20 patients (53%) had a light touch deficit, 19 (50%) had a pressure deficit, 17 (45%) had a deficit in pinprick sensation, and 19 (50%) had impaired proprioception. Finally, deficits in the perceptual threshold of touch were present in 65% of the patients, whereas 23% had impaired SSEP. Further detailed information on the patient characteristics is shown in Table 1.

Table 1
Patient characteristics (n = 38).

Age stroke onset, years: median (IQR)	74.7 (62.8–80.6)
Gender, n (%)	38 (100)
Male	20 (52.6)
Female	18 (47.4)
Days after stroke, median (IQR)	6 (5–7)
Affected hemisphere, n (%)	
Left	10 (26.3)
Right	28 (73.7)
Type of stroke, n (%)	
Ischemia	33 (86.8)
Hemorrhage	5 (13.2)
Hand dominance, n (%)	
Left	1 (3)
Right	37 (97)
Stroke severity (NIHSS): median (SD)	8.5 (6–13)
Visuo-spatial neglect, n (%)[a]	8 (22.9)
Em-NSA-light touch (/8): median (IQR)	6 (0–8)
Em-NSA-pressure (/8): median (IQR)	7 (2–8)
Em-NSA-pinprick (/8): median (IQR)	8 (3–8)
Em-NSA- proprioception (/8): median (IQR)	6.5 (3.75–8)
Deficit in all 4 Em-NSA subscales	16 (42)
Deficit in 1, 2, or 3 Em-NSA subscales	6 (16)
No deficit in Em-NSA subscales	16 (42)
PTT deficit: n (%)[b]	24 (64.9)
SSEP deficit: n (%)[c]	7 (23.3)

IQR: interquartile range, NIHSS: National Institutes of Health Stroke Scale, Em-NSA: Erasmus MC modification of the (revised) Nottingham sensory assessment, PTT: perceptual threshold of touch, SSEP: somatosensory evoked potentials.
[a] Missing values n = 3.
[b] Missing values n = 1.
[c] Missing values n = 8.

The overlay of the stroke lesions of all patients showed a wide distribution across the entire hemisphere including all four brain lobes and the brain stem. In particular, the coalescing of lesion sites confirmed the majority had middle cerebral artery territory lesions. Subcortical areas such as corona radiata, extreme, external, and internal capsule, claustrum, basal ganglia, thalamus, as well as insular and opercular cortex were most frequently involved (Fig. 1).

Fig. 2 shows the statistical maps of the VLSM analysis of the four Em-NSA subscales. Lesions in the parietal subcortical white matter, the dorsal internal capsule, and in the insular and opercular cortex were associated with deficits in all four somatosensory modalities (Table 2). The extent and distribution of significant voxels, however, differed slightly between the four Em-NSA tests. The largest area of significant voxels covering 18.5 ml was found for light touch deficits including the parietal white matter parts of the corona radiata inferior to the post- and precentral gyri, the parietal operculum, the insular cortex, and the external, dorsal internal, and extreme capsule. Significant voxels associated to a pressure deficit comprised a volume of 9.7 ml including similar regions as for light touch, but with lesser involvement of the frontal parts of the external and extreme capsule and the insular cortex. Maximal association was found in the parietal operculum and the parietal white matter of the corona radiata, inferior to the post- and precentral gyrus. Voxels associated with pinprick deficits were found in the parietal operculum as well as in parts of the insular cortex and the white matter inferior to the post- and precentral gyri comprising a volume of 2.9 ml. Finally, the test for proprioception deficit identified the smallest number of voxels adding up to a volume of 1.4 ml, including the corona radiata inferior to the post- and precentral gyrus as well as small parts of the parietal opercular and the dorsal insular cortex (Table 2). Overlay maps of voxels contributing to symptoms in the four somatosensory modalities identified two brain regions showing significant associations in all four tests: the white matter in parietal
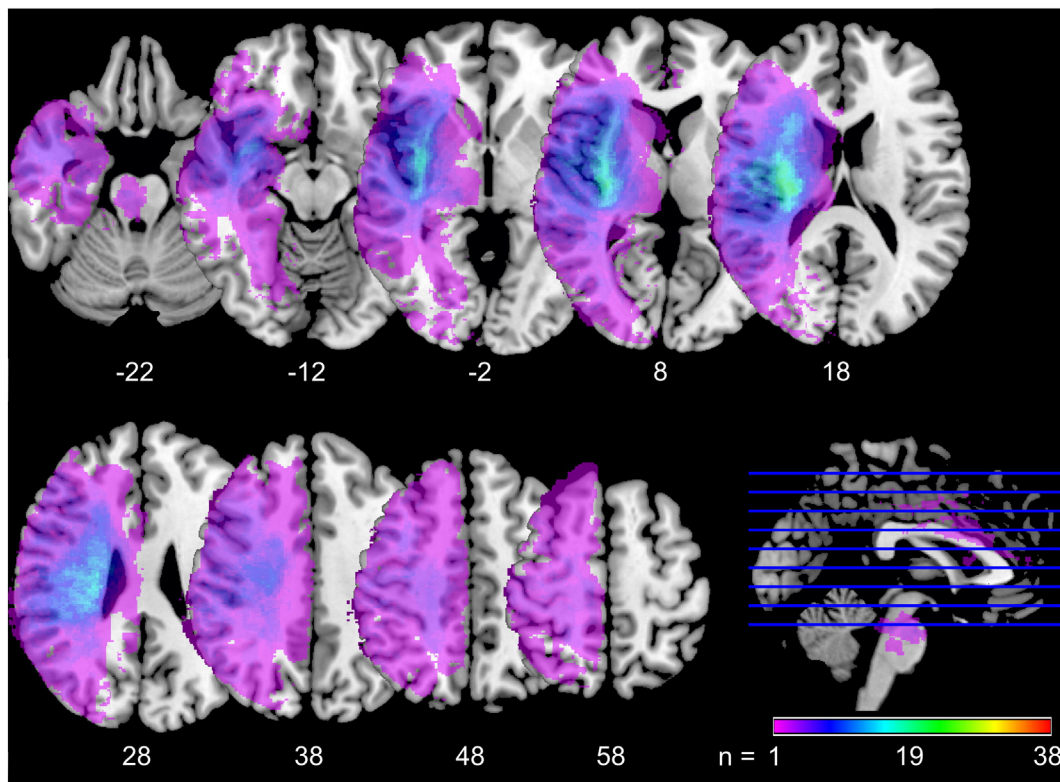

Fig. 1. Lesion overlay plot. Fig. 1 shows an overlay map of individual stroke lesions of all 38 patients. Maps are overlaid on a T1-template in MNI space $1 \times 1 \times 1$ mm³. All lesions were flipped to the right hemisphere. MNI coordinates of each transverse section (z-axis) and a sagittal slice for visualization are given. Color scale indicates the number of patients having a lesion in this voxel. Stroke lesions are distributed across the entire hemisphere. Most frequently lesioned voxels are found in the insula, the corona radiata, and in the striatocapsular region. (For interpretation of the references to color in this figure legend, the reader is referred to the web version of this article.)
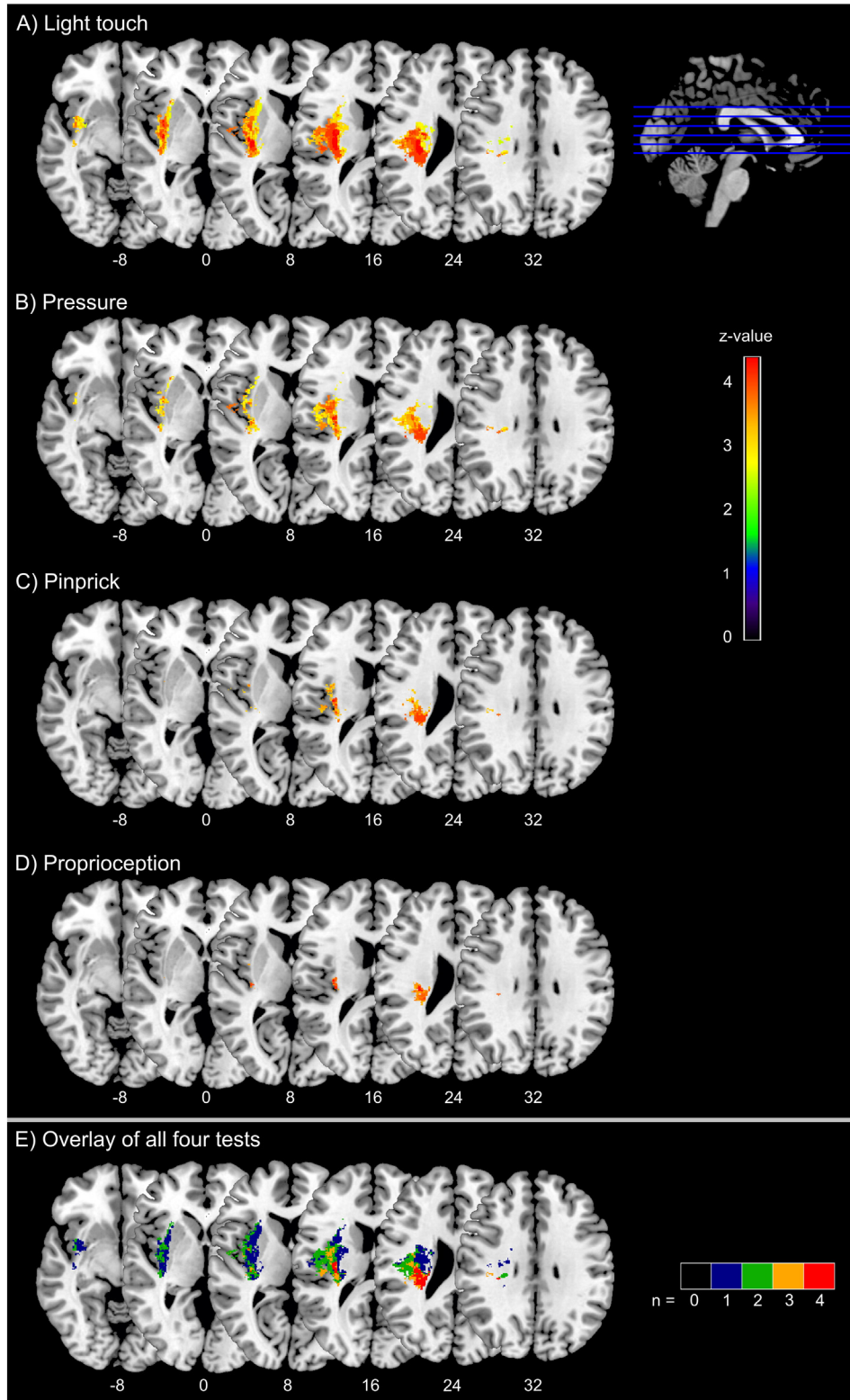
Fig. 2. Voxel-based statistical analysis of lesion impact on somatosensory deficit of light touch, pressure, pinprick, and proprioception. Fig. 2 shows results from voxel-based lesion-symptom mapping displaying voxels with significant association in lesion-symptom mapping to four somatosensory tests: 2A) light touch, 2B) pressure, 2C) pinprick, and 2D) proprioception. Color scale indicates Brunner–Munzel rank order z-statistics. All tests are corrected for multiple comparisons at a level of 1% FDR. Statistical maps are overlaid on a T1-template in MNI space $1 \times 1 \times 1$ mm^3. MNI coordinates of each transverse section (z-axis) and a sagittal slice for visualization are given. Distribution of significant voxels slightly differs between the four tests. However, in all tests there is a significant contribution of voxels in the secondary somatosensory cortex, the insular cortex, the dorsal internal capsule, and the thalamocortical pathway to tested somatosensory deficits. 2E shows an overlay of all four tests. Color scale indicates for each voxel the number of somatosensory tests for which a significant association was seen in case of a lesion in this voxel. Two core regions can be identified showing a relation to all four somatosensory modalities (red voxels): the white matter in parietal lobe near the central region and the parietal operculum close to the insular cortex. (For interpretation of the references to color in this figure legend, the reader is referred to the web version of this article.)

Table 2
Stroke lesion locations associated with somatosensory deficits.

Tested symptom	MNI coordinates (mm)			Brain region	Z-score
	X	Y	Z		
Light touch	29	−25	25	Superior thalamocortical radiation	7.2**
	34	−7	18	S2/parietal operculum	7.1**
	34	−14	16	Insulo-opercular cortex	6.8**
	29	−23	25	STR	6.6**
	33	−5	13	External capsule	6.2**
	33	−19	21	S2/parietal operculum	5.1**
	35	−15	16	S2/parietal operculum	3.9**
	42	−35	27	Inferior parietal lobule	3.9**
	28	−21	12	CST	3.5**
	28	−5	10	Putamen	3.2**
	27	−19	14	Posterior limb of internal capsule	3.1**
Pressure	34	−14	16	Insulo-opercular cortex	4.9**
	29	−25	25	STR	4.8**
	32	−22	23	S2/parietal operculum	4.0**
	35	2	2	External capsule	3.7**
	29	−21	12	Posterior limb of internal capsule	3.4**
	37	−12	12	Insular cortex	3.1**
	46	−14	18	S2/parietal operculum	3.1**
	28	−21	12	CST	3.1**
	30	−6	12	Putamen	2.7**
Pinprick	32	−22	23	S2/parietal operculum	4.3**
	29	−25	25	STR	4.3**
	34	−15	16	Insulo-opercular cortex	4.2**
	29	−21	23	CST	3.7**
	42	−35	27	Inferior parietal lobule	3.7**
	29	−21	12	Posterior limb of internal capsule	3.1**
	35	2	2	External capsule	2.6**
Proprioception	32	−20	15	S2/parietal operculum	4.6**
	29	−25	25	STR	4.6**
	34	−14	16	Insulo-opercular cortex	4.4**
	32	−21	17	S2/parietal operculum	3.9**
	27	−21	24	CST	3.7**
PTT	34	−14	15	Insulo-opercular cortex	−4.0++
	34	−6	15	S2/parietal operculum	−3.9++
	31	−22	18	S2/parietal operculum	−3.9++
	29	−24	25	STR	−3.5++
	36	−13	2	External capsule	−3.2++
	31	5	5	Putamen	−3.0++
SSEP	30	−12	14	S2/parietal operculum	−3.7+
	29	−24	25	STR	−3.7+
	34	−17	16	S2/parietal operculum	−3.4+
	29	−16	12	Posterior limb of internal capsule	−3.2+
	35	3	2	External capsule	−2.3+

PTT = perceptual threshold of touch, SSEP = somatosensory evoked potentials, S2 = secondary somatosensory cortex, STR = superior thalamocortical radiation, CST = corticospinal tract. All given brain regions are corrected for multiple comparison. If indicated with two asterisks (**), the voxel is tested significant based on Brunner–Munzel Z-score after applying a FDR of 0.01. For dichotomous variables, Liebermeister Z-scores are indicated with a double cross (++) for FDR 0.01 or a single cross (+) for FDR 0.05.

lobe near the central region (maximum in the MNI-coordinate 29/−25/25 mm) and the parietal operculum close to the insular cortex (maximum in the MNI-coordinate 35/−15/16 mm) (see Fig. 2).

Probabilistic fiber tracking demonstrated that the parietal subcortical white matter region shows strong connections to projection fibers from the dorsal brain stem through the dorsal internal capsule and thalamus up to the postcentral gyrus (Fig. 3, golden tract). This pathway matches the anatomical course of the ascending sensory tract. In addition, a frontal associative connection along the external capsule and a connection to the cerebellum could be identified (Fig. 3, golden tract). The structural connectivity of the second, opercular region revealed an association pathway from the thalamus to the parietal operculum and the insular cortex which corresponds to sensory fibers from thalamus to the secondary somatosensory cortex as well as connections to the primary somatosensory cortex (Fig. 3, green tract).

The VLSM analysis of the PTT and SSEP showed a similar pattern of lesion distribution with significant association to abnormalities in

these tests (Fig. 4). Voxels from the parietal opercular cortex, the insular cortex, the internal and external capsule and the thalamocortical tract showed association to a deficit in PTT. Voxels in the thalamocortical tract showed an association to deficits in SSEP (Table 2).

4. Discussion

In this voxel-based lesion-symptom mapping study we investigated which brain regions are important in the occurrence of exteroceptive and proprioceptive somatosensory deficits in the upper limb in the early phase post stroke. Although we observed a slight difference in extent and distribution of contributing voxels for deficits to the different somatosensory modalities, the analysis showed that lesions in two core brain regions were associated with both exteroceptive and proprioceptive deficits in the arm and hand post stroke: the parietal subcortical white matter near the postcentral region and the parietal operculum close to the insular cortex. The anatomical localization of the parietal subcortical cluster (MNI coordinate 29/−25/25) corresponds to the sensory component of the superior thalamic radiation (sSTR) and thus represents the afferent sensory thalamocortical tract (Borstad et al., 2012). The second cluster in the parietal operculum (MNI coordinate 35/−15/16) close to the dorsal insular cortex corresponds functionally to the secondary somatosensory cortex (Eickhoff et al., 2006b).

Our results are well in line with VLSM-findings from Preusser and colleagues who identified the parietal operculum, together with the insular cortex, putamen, and subcortical connections reaching towards the prefrontal cortex to be causally involved in the perception of touch (Preusser et al., 2014). They highlighted the contribution of anterior parts of the parietal operculum (OP 4 and OP 3), which matches our findings including not only the parietal white matter but also parts of the insula to be related to light touch processing. Our peak cluster at MNI coordinate 35/-15/16 is situated in the border zone of the second and third regions of the parietal operculum (OP 2, maximum probability at 36/−24/23; OP 3, maximum probability at 42/−15/23), and to a lesser extent in the fourth region (OP 4, maximum probability at 60/−12/19) (Eickhoff et al., 2006a). In contrast to the study of Preusser and colleagues who included a young cohort (mean age 46) of patients in the chronic stage of stroke (12 to 16 months after onset), we investigated both multiple exteroceptive and proprioceptive deficits in the acute stroke phase. Our results for pressure, pinprick, and proprioception showed similar involvement of the parietal white matter and the insulo-opercular cortex, however the amount of frontal insular voxels was less pronounced for proprioception. Thus, our study adds to the current knowledge that these brain areas are not only involved in the perception of touch, but are also important in the perception of pressure, pinprick and movement sense, especially in the early phase post stroke. While there were small differences in the extent and distribution of contributing voxels between the different somatosensory deficits, the overall pattern of lesion-deficit inference was similar. Therefore, a novel finding of this study is that different somatosensory modalities are affected by stroke lesions in the same brain areas.

The slight differences of significant voxels sites between light touch, pressure, pinprick and proprioception may be explained by two facts: first, the random statistical variance in our sample. For the multiple comparison correction, a higher cut-off level of significance had to be applied for proprioception compared to light touch. In detail, the cut-off z-value for the FDR-correction of 1% was 2.3867 for light touch, whereas for pinprick it was 2.9999. This may have led to a smaller amount of significant voxels for the pinprick modality. A second, more clinical and anatomical explanation might be that the modality of light touch may be more susceptible to impairment after stroke compared to pressure, pinprick or proprioception. The latter modalities include a more pronounced stimulus compared to light touch and are therefore called more robust modalities. In other words, from the anatomical point of view one could assume that if only parts at the border of the ascending somatosensory tract in the white matter are lesioned, then only
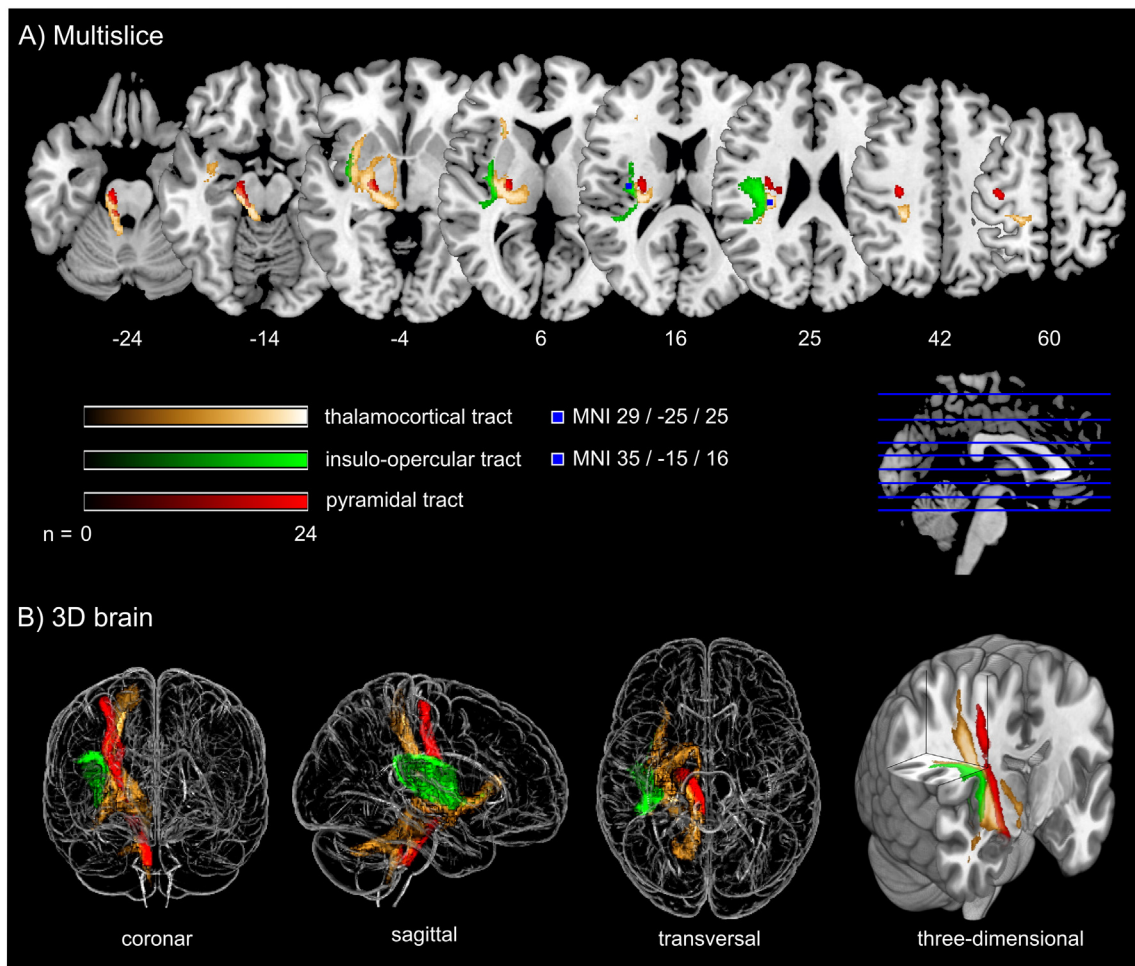
Fig. 3. Fiber tracking results starting from core brain regions in 24 age-matched healthy controls. Fig. 3 shows three different probabilistic fiber tracts, taken from 24 healthy age-matched volunteers demonstrating structural connectivity of the two core regions of somatosensory lesion-symptom mapping in relation to the pyramidal tract. The golden and the green pathway were tracked based on the VLSM results from the somatosensory tests (Fig. 2): the two peak coordinates from the two core regions showing an overlap in VLSM-analysis for all four somatosensory modalities were entered as seed coordinates for probabilistic fiber tracking (MNI coordinates 29/−25/25 and 35/−15/16). For anatomical comparison, the pyramidal tract is shown in red color. In A), maps are overlaid on a T1-template in MNI space $1 \times 1 \times 1$ mm^3. MNI coordinates of each transverse section (z-axis) and a sagittal slice for visualization are given. Color scales indicate the number of volunteers presenting the tract in this voxel. The two blue squares in transverse sections (z = 16 and z = 25) display the seed coordinates which were taken for the fiber tracking. In B), a 'glass brain' visualization and a half-split three-dimensional model of the three tracts is shown. (For interpretation of the references to color in this figure legend, the reader is referred to the web version of this article.)

light touch may be impaired. In contrast, if the entire somatosensory tract is lesioned, also other tactile modalities will be deficient. This corresponds to the slight shift we see in Fig. 2 for the four different somatosensory modalities: lesion sites significantly associated to light touch deficit cover a greater area compared to the other modalities. Importantly, all four modalities have their peak values in the same key areas. We further are the first to confirm results from clinical somatosensory assessments by quantitative measurements of exteroception and proprioception through recordings of the perceptual threshold of touch and somatosensory evoked potentials, respectively.

Our findings from probabilistic fiber tracking in healthy age-matched controls support that the two core brain regions identified by the VLSM analysis, in which lesions lead to both exteroceptive and proprioceptive deficits, have different projections to somatosensory-processing areas within the CNS. Both of the pathways seem to be involved in multimodal somatosensory processing. First, the parietal subcortical white matter cluster is in close relationship with the sensory component of the superior thalamic radiation (sSTR). Indeed, it showed strong connections to projection fibers from the dorsal brain stem through the dorsal internal capsule and thalamus up to the primary somatosensory cortex (postcentral gyrus). The relationship between post-stroke somatosensory ability and structural integrity of the sSTR has been determined previously (Borstad et al., 2012). Additionally to this

projection, a frontal associative connection was found along the external capsule. This tract is very close to the ventral pathway described by Preusser and colleagues. Furthermore, a cerebellar pathway diverging from the main tract was found, usually containing sensory spinocerebellar fibers (Nieuwenhuys et al., 2008). Second, the structural connectivity of the parietal opercular region revealed an association pathway between the parietal operculum, the insular cortex, the thalamus and the subcortical parietal white matter below the postcentral gyrus. This pathway contains sensory fibers from thalamus to the secondary somatosensory cortex reaching to the insular cortex as well as associative fibers between primary and secondary somatosensory cortex. Structural connections from ventroposterior lateral and inferior thalamic nuclei to secondary somatosensory cortex have been described previously (Behrens et al., 2003; Eickhoff et al., 2010). Furthermore, strong structural and functional connectivity between S2 and posterior insular cortex has been reported (Wiech et al., 2014).

The insular cortex, anatomically located between the temporal, the frontal, and the parietal lobe, is considered to be a multimodal sensory integrative area (Mazzola et al., 2012). The anterior and the posterior part of the insular cortex seem to have different functions. The anterior insular cortex plays a role in processing visceral sensation, the so called interoception (Fowler, 2003) and in cognitive–affective aspects of pain perception (Wiech et al., 2010). The anterior part is further linked to
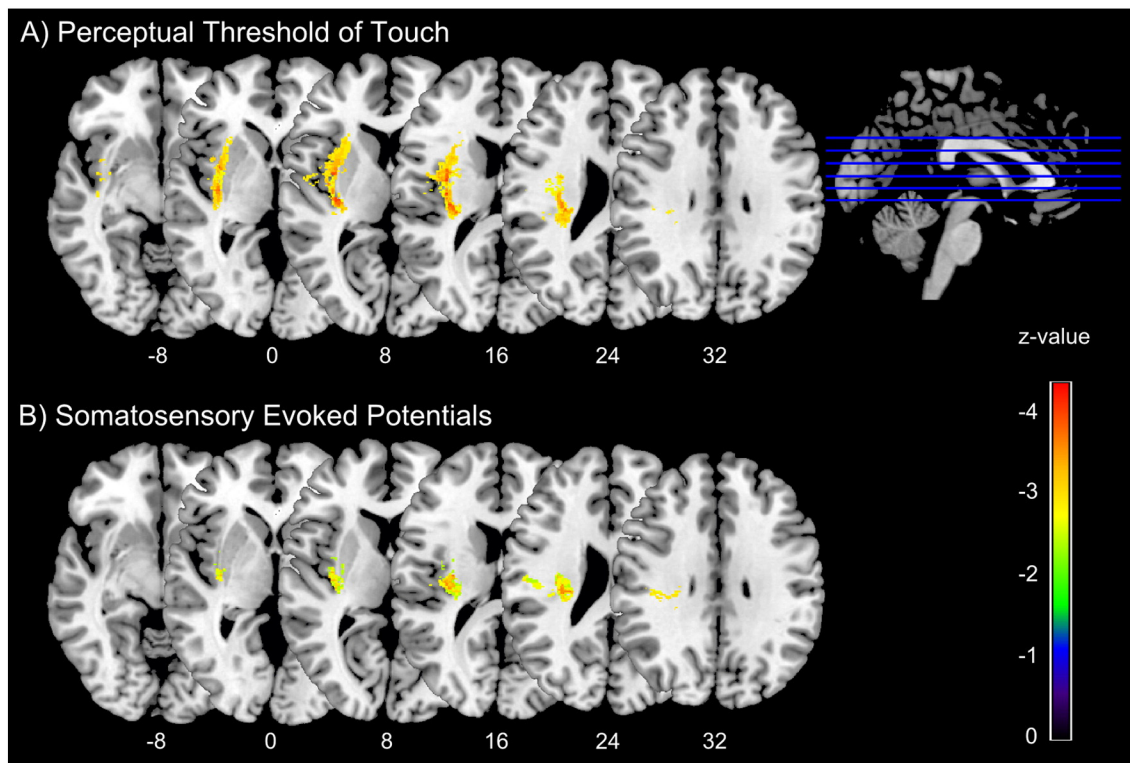
Fig. 4. Voxel-based statistical analysis of lesion impact on perceptual threshold of touch and somatosensory evoked potentials. Fig. 4 shows significant voxels from lesion-symptom mapping for A) the *perceptual threshold of touch* and B) *somatosensory evoked potentials*, based on Liebermeister statistical test. Color scale indicates z-statistics. For test A) results are corrected for multiple comparisons at a level of 1% FDR. For exploratory reasons in the SSEP analysis, results are corrected on a more liberal threshold (5% FDR), to account for the large amount of missing values. Statistical maps are overlaid on a T1-template in MNI space $1 \times 1 \times 1$ mm^3. MNI coordinates of each transverse section (z-axis) and a sagittal slice for visualization are given. (For interpretation of the references to color in this figure legend, the reader is referred to the web version of this article.)

body awareness (Critchley et al., 2004) and has been even referred to as a neural correlate of consciousness (Craig, 2009). In contrast, the dorsal insular cortex might represent a somatosensory association area (Karnath and Baier, 2010), being involved in processing of different exteroceptive functions. There is emerging evidence that the dorsal insular cortex is specifically involved in the perception of pain (Kessner et al., 2014; Tracey, 2011) and in the magnitude of perceived pain (Baliki et al., 2009). Abnormal pain thresholds are reported in patients with stroke lesion in the posterior insular cortex (Greenspan et al., 1999). Mazolla and colleagues showed that there is a somatotopic organization in the human operculo-insular cortex with diverse activation patterns in response to different somatosensory stimuli (Mazzola et al., 2012). In a small sample of patients with insular strokes, Baier and colleagues demonstrated by VLSM that insular stroke lesions are associated with impaired temperature perception (Baier et al., 2014). In our study, we could demonstrate an expanded function of the posterior insular cortex, which was significantly associated to deficits in light touch, pressure, pinprick, and proprioception, underpinning the multimodal integrative function of the insula. Thereby our findings support the involvement of the dorsal insular cortex in processing of exteroception and proprioception, in contrast to the anterior insular cortex which has been previously referred to as being important for interoception (Fowler, 2003).

A few limitations of our study need to be addressed. First, to increase the generalizability of this study, we did not exclude patients with visuo-spatial neglect. Neglect is the inability to detect and respond to stimuli occurring in the hemi-space contralateral to a brain lesion, most commonly after right-hemisphere stroke (Heilman and Valenstein, 1979). In the present study, the number of patients with neglect was too small to draw conclusions about the correlation of neglect, somatosensory deficits and the corresponding brain regions that were affected. However, it is commonly alleged that brain regions important in somatosensory processing are in close proximity to brain regions

responsible for neglect. Lesions affecting the superior and middle temporal gyrus, the temporo-parietal junction, the intraparietal sulcus and the insular cortex were found to be associated with spatial neglect. Also, the basal ganglia, especially putamen and caudate nucleus, the thalamus, and paraventricular white matter structures underlying the inferior parietal cortex were associated with neglect (De Schotten et al., 2014; Karnath et al., 2004, 2011). Therefore, neglect might have interfered with the somatosensory assessment due to the attention deficit. Importantly, we also recruited patients with visuo-spatial neglect who did not have any somatosensory deficit, which supports the notion that somatosensory function in patients with visuo-spatial neglect can be tested and the somatosensory assessment is valid. Furthermore, it is reassuring that our results are well in line with VLSM-findings from Preusser et al. (2014) who excluded patients with visuo-spatial neglect in their study. Second, to increase statistical power of identifying lesion patterns, all lesion maps were flipped onto the right hemisphere. Therefore, hemisphere-specific information could not be studied, but we also did not have any hypothesis on lateralized processing of somatosensation. In our sample there was a bias regarding the side of the affected hemisphere that lead to more patients having a right hemisphere lesion. This was due to the fact that patients with left hemisphere stroke are more likely to have severe aphasia, which were excluded from the study. Furthermore, in the VLSM statistics, only voxels that were lesioned in at least ten patients could be investigated. Therefore, voxels tested in this analysis did not include some important brain regions for somatosensory processing such as the brainstem, thalamus and primary somatosensory cortex. Since the patients had stroke lesions, a selection bias towards brain lesions that correlate with vascular territories cannot be ruled out. Furthermore, both patients with ischemic infarction and hemorrhagic stroke were included. Although the stroke etiology is very different, it does not affect the VLSM statistics, and it further enhances generalizability of our results to the broader

stroke population. Lastly, probabilistic tractography offers the advantage of modeling multiple fiber orientations to detect a range of subordinate pathways missed by deterministic fiber tracking. However, normalization of tractography to remove false-positive results is not standardized and remains arbitrary to some extent and has been discussed as a potential limitation previously (Behrens et al., 2007).

In summary, this VLSM study provides evidence that the sensory component of the superior thalamocortical radiation towards the postcentral gyrus is one of the most vulnerable brain regions to cause somatosensory deficits if lesioned by stroke. Furthermore, we endorse previous findings on the importance of the parietal operculum and insular cortex to somatosensory processing. The novel aspect of the present study is the combination of both voxel-based lesion-symptom mapping and probabilistic fiber tracking to investigate the relationship between different somatosensory deficits, measured with both standardized clinical assessment and more objective measures, and the underlying structural brain regions in a representative sample of patients with acute stroke. We found that similar lesion patterns are associated with multiple deficits in different somatosensory modalities in the upper limb. Future research should address the longitudinal somatosensory assessment with respect to lesion-symptom associations and the clinical question, to which extent somatosensory deficits can be regained during rehabilitation according to lesion localization.

Author contributions

S.M. and S.S.K. contributed equally to this work. All other authors have participated in the conception of the study, the data analysis, and editing of the manuscript.

Conflicts of interest

The authors declare no conflicts of interest.

Acknowledgments

Appendix A. Supplementary data

Supplementary data to this article can be found online at http://dx.doi.org/10.1016/j.nicl.2015.12.005.

References

American Clinical Neurophysiology Society, 2006. Guideline 9D: guidelines on short-latency somatosensory evoked potentials. J. Clin. Neurophysiol. 23, 168–179.

Baier, B., Zu Eulenburg, P., Geber, C., Rohde, F., Rolke, R., Maihöfner, C., Birklein, F., Dieterich, M., 2014. Insula and sensory insular cortex and somatosensory control in patients with insular stroke. Eur. J. Pain 18, 1385–1393. http://dx.doi.org/10.1002/j.1532-2149.2014.501.x.

Baliki, M.N., Geha, P.Y., Apkarian, A.V., 2009. Parsing pain perception between nociceptive representation and magnitude estimation. J. Neurophysiol. 101, 875–887. http://dx.doi.org/10.1152/jn.91100.2008.

Behrens, T.E.J., Johansen-Berg, H., Woolrich, M.W., Smith, S.M., Wheeler-Kingshott, C.A.M., Boulby, P.A., Barker, G.J., Sillery, E.L., Sheehan, K., Ciccarelli, O., Thompson, A.J., Brady, J.M., Matthews, P.M., 2003. Non-invasive mapping of connections between human thalamus and cortex using diffusion imaging. Nat. Neurosci. 6, 750–757. http://dx.doi.org/10.1227/01.NEU.0000309595.77090.89.

Behrens, T.E.J., Berg, H.J., Jbabdi, S., Rushworth, M.F.S., Woolrich, M.W., 2007. Probabilistic diffusion tractography with multiple fibre orientations: what can we gain? NeuroImage 34, 144–155. http://dx.doi.org/10.1016/j.neuroimage.2006.09.018.

Borstad, A., Schmalbrock, P., Choi, S., Nichols-Larsen, D.S., 2012. Neural correlates supporting sensory discrimination after left hemisphere stroke. Brain Res. 1460, 78–87. http://dx.doi.org/10.1016/j.brainres.2012.03.060.

Burton, H., Jones, E.G., 1976. The posterior thalamic region and its cortical projection in New World and Old World monkeys. J. Comp. Neurol. 168, 249–301. http://dx.doi.org/10.1002/cne.901680204.

Carey, L.M., Matyas, T.A., 2011. Frequency of discriminative sensory loss in the hand after stroke in a rehabilitation setting. J. Rehabil. Med. 43, 257–263. http://dx.doi.org/10.2340/16501977-0662.

Cheng, B., Forkert, N.D., Zavaglia, M., Hilgetag, C.C., Golsari, A., Siemonsen, S., Fiehler, J., Pedraza, S., Puig, J., Cho, T.-H., Alawneh, J., Baron, J.-C., Ostergaard, L., Gerloff, C., Thomalla, G., 2014. Influence of stroke infarct location on functional outcome measured by the modified rankin scale. Stroke 45, 1695–1702. http://dx.doi.org/10.1161/STROKEAHA.114.005152.

Chiappa, K., 2003. Evoked Potentials in Clinical Medicine. Williams & Wilkins, Philadelphia.

Connell, L.A., Lincoln, N.B., Radford, K.A., 2008. Somatosensory impairment after stroke: frequency of different deficits and their recovery. Clin. Rehabil. 22, 758–767. http://dx.doi.org/10.1177/0269215508090674.

Craig, A.D.B., 2009. How do you feel—now? The anterior insula and human awareness. Nat. Rev. Neurosci. 10, 59–70. http://dx.doi.org/10.1038/nrn2555.

Critchley, H.D., Wiens, S., Rotshtein, P., Ohman, A., Dolan, R.J., 2004. Neural systems supporting interoceptive awareness. Nat. Neurosci. 7, 189–195. http://dx.doi.org/10.1038/nn1176.

De Schotten, M.T., Tomaiuolo, F., Aiello, M., Merola, S., Silvetti, M., Lecce, F., Bartolomeo, P., Doricchi, F., 2014. Damage to white matter pathways in subacute and chronic spatial neglect: a group study and 2 single-case studies with complete virtual "in vivo" tractography dissection. Cereb. Cortex 24, 691–706. http://dx.doi.org/10.1093/cercor/bhs351.

DeJong, R., 1979. The neurologic examination. Philadelphia. Harper & Row, pp. 178–198.

Dijkerman, H.C., de Haan, E.H.F., 2007. Somatosensory processes subserving perception and action. Behav. Brain Sci. 30, 189–239. http://dx.doi.org/10.1017/S0140525X07001392.

Eek, E., Engardt, M., 2003. Assessment of the perceptual threshold of touch (PTT) with high-frequency transcutaneous electric nerve stimulation (Hf/TENS) in elderly patients with stroke: a reliability study. Clin. Rehabil. 17, 825–834. http://dx.doi.org/10.1191/0269215503cr640oa.

Eek, E., Holmqvist, L.W., Sommerfeld, D.K., 2012. Adult norms of the perceptual threshold of touch (PTT) in the hands and feet in relation to age, gender, and right and left side using transcutaneous electrical nerve stimulation. Physiother. Theory Pract. 28, 373–383. http://dx.doi.org/10.3109/09593985.2011.629021.

Eickhoff, S.B., Amunts, K., Mohlberg, H., Zilles, K., 2006a. The human parietal operculum. II. Stereotaxic maps and correlation with functional imaging results. Cereb. Cortex 16, 268–279. http://dx.doi.org/10.1093/cercor/bhi106.

Eickhoff, S.B., Schleicher, A., Zilles, K., Amunts, K., 2006b. The human parietal operculum. I. Cytoarchitectonic mapping of subdivisions. Cereb. Cortex 16, 254–267. http://dx.doi.org/10.1093/cercor/bhi105.

Eickhoff, S.B., Jbabdi, S., Caspers, S., Laird, A.R., Fox, P.T., Zilles, K., Behrens, T.E.J., 2010. Anatomical and functional connectivity of cytoarchitectonic areas within the human parietal operculum. J. Neurosci. 30, 6409–6421. http://dx.doi.org/10.1523/JNEUROSCI.5664-09.2010.

Forkert, N.D., Cheng, B., Kemmling, A., Thomalla, G., Fiehler, J., 2014. ANTONIA perfusion and stroke. A software tool for the multi-purpose analysis of MR perfusion-weighted datasets and quantitative ischemic stroke assessment. Methods Inf. Med. 53, 469–481. http://dx.doi.org/10.3414/ME14-01-0007.

Fowler, C.J., 2003. Visceral sensory neuroscience: interoception. Brain 126, 1505–1506. http://dx.doi.org/10.1093/brain/awg120.

Friedman, P.J., 1992. The star cancellation test in acute stroke. Clin. Rehabil. 6, 23–30. http://dx.doi.org/10.1177/026921559200600104.

Georgiadis, A.L., Yamamoto, Y., Kwan, E.S., Pessin, M.S., Caplan, L.R., 1999. Anatomy of sensory findings in patients with posterior cerebral artery territory infarction. Arch. Neurol. 56, 835–838. http://dx.doi.org/10.1001/archneur.56.7.835.

Greenspan, J.D., Lee, R.R., Lenz, F.A., 1999. Pain sensitivity alterations as a function of lesion location in the parasylvian cortex. Pain 81, 273–282. http://dx.doi.org/10.1016/S0304-3959(99)00021-4.

Heilman, K.M., Valenstein, E., 1979. Mechanisms underlying hemispatial neglect. Ann. Neurol. 5, 166–170. http://dx.doi.org/10.1002/ana.410050210.

Jenkinson, M., Beckmann, C.F., Behrens, T.E.J., Woolrich, M.W., Smith, S.M., 2012. FSL. NeuroImage 62 (2), 782–790. http://dx.doi.org/10.1016/j.neuroimage.2011.09.015.

Karnath, H.O., Baier, B., 2010. Right insula for our sense of limb ownership and self-awareness of actions. Brain Struct. Funct. 214, 411–417. http://dx.doi.org/10.1007/s00429-010-0250-4.

Karnath, H.O., Berger, M.F., Küker, W., Rorden, C., 2004. The anatomy of spatial neglect based on voxelwise statistical analysis: a study of 140 patients. Cereb. Cortex 14, 1164–1172. http://dx.doi.org/10.1093/cercor/bhh076.

Karnath, H.-O., Rennig, J., Johannsen, L., Rorden, C., 2011. The anatomy underlying acute versus chronic spatial neglect: a longitudinal study. Brain 134, 903–912. http://dx.doi.org/10.1093/brain/awq355.

Kessner, S., Forkmann, K., Ritter, C., Wiech, K., Ploner, M., Bingel, U., 2014. The effect of treatment history on therapeutic outcome: psychological and neurobiological underpinnings. PLoS One 9, e109014. http://dx.doi.org/10.1371/journal.pone.0109014.

Kim, J.S., 1992. Pure sensory stroke. Clinical–radiological correlates of 21 cases. Stroke 23, 983–987. http://dx.doi.org/10.1161/01.STR.23.7.983.

Lindell, A.B., Jalas, M.J., Tenovuo, O., Brunila, T., Voeten, M.J.M., Hämäläinen, H., 2007. Clinical assessment of hemispatial neglect: evaluation of different measures and dimensions. Clin. Neuropsychol. 21, 479–497. http://dx.doi.org/10.1080/13854040600630061.

Martin, J., Jessel, T., 1991. Anatomy of the somatic sensory system. In: Kandel, Schwartz, Jessel (Eds.), Principles of Neural Science. Elsevier, New York, pp. 353–366.

Mazzola, L., Faillenot, I., Barral, F.G., Mauguière, F., Peyron, R., 2012. Spatial segregation of somato-sensory and pain activations in the human operculo-insular cortex. NeuroImage 60, 409–418. http://dx.doi.org/10.1016/j.neuroimage.2011.12.072.

Medina, J., Kimberg, D.Y., Chatterjee, A., Coslett, H.B., 2010. Inappropriate usage of the Brunner–Munzel test in recent voxel-based lesion-symptom mapping studies. Neuropsychologia 48, 341–343. http://dx.doi.org/10.1016/j.neuropsychologia.2009.09.016.

Meyer, S., Karttunen, A.H., Thijs, V., Feys, H., Verheyden, G., 2014. How do somatosensory deficits in the arm and hand relate to upper limb impairment, activity, and participation problems after stroke? A systematic review. Phys. Ther. 94, 1220–1231. http://dx.doi.org/10.2522/ptj.20130271.

Nieuwenhuys, R., Voogd, J., van Huijzen, C., 2008. The human central nervous system. 4th ed. Am. J. Neuroradiol. http://dx.doi.org/10.3174/ajnr.A0991.

Oostenveld, R., Praamstra, P., 2001. The five percent electrode system for high-resolution EEG and ERP measurements. Clin. Neurophysiol. 112, 713–719. http://dx.doi.org/10.1016/S1388-2457(00)00527-7.

Preusser, S., Thiel, S.D., Rook, C., Roggenhofer, E., Kosatschek, A., Draganski, B., Blankenburg, F., Driver, J., Villringer, A., Pleger, B., 2014. The perception of touch and the ventral somatosensory pathway. Brain 138, 540–548. http://dx.doi.org/10.1093/brain/awu370.

Rabin, E., Gordon, A.M., 2004. Tactile feedback contributes to consistency of finger movements during typing. Exp. Brain Res. 155, 362–369. http://dx.doi.org/10.1007/s00221-003-1736-6.

Rehme, A.K., Eickhoff, S.B., Rottschy, C., Fink, G.R., Grefkes, C., 2012. Activation likelihood estimation meta-analysis of motor-related neural activity after stroke. NeuroImage 59, 2771–2782. http://dx.doi.org/10.1016/j.neuroimage.2011.10.023.

Rorden, C., Karnath, H.-O., Bonilha, L., 2007. Improving lesion-symptom mapping. J. Cogn. Neurosci. 19, 1081–1088. http://dx.doi.org/10.1162/jocn.2007.19.7.1081.

Sherrington, C.S., 1907. On the proprio-ceptive system, especially in its reflex aspect. Brain 29, 467–482. http://dx.doi.org/10.1093/brain/29.4.467.

Stolk-Hornsveld, F., Crow, J.L., Hendriks, E.P., van der Baan, R., Harmeling-van der Wel, B.C., 2006. The Erasmus MC modifications to the (revised) Nottingham Sensory Assessment: a reliable somatosensory assessment measure for patients with intracranial disorders. Clin. Rehabil. 20, 160–172.

Tracey, I., 2011. Can neuroimaging studies identify pain endophenotypes in humans? Nat. Rev. Neurol. 7, 173–181. http://dx.doi.org/10.1038/nrneurol.2011.4.

Tyson, S.F., Hanley, M., Chillala, J., Selley, A.B., Tallis, R.C., 2008. Sensory loss in hospital-admitted people with stroke: characteristics, associated factors, and relationship with function. Neurorehabil. Neural. Repair 22, 166–172. http://dx.doi.org/10.1177/1545968307305523.

Ward, N.S., Brown, M.M., Thompson, A.J., Frackowiak, R.S.J., 2003. Neural correlates of motor recovery after stroke: a longitudinal fMRI study. Brain 126, 2476–2496. http://dx.doi.org/10.1093/brain/awg245.

Wiech, K., Lin, C., Brodersen, K.H., Bingel, U., Ploner, M., Tracey, I., 2010. Anterior insula integrates information about salience into perceptual decisions about pain. J. Neurosci. 30, 16324–16331. http://dx.doi.org/10.1523/JNEUROSCI.2087-10.2010.

Wiech, K., Jbabdi, S., Lin, C.S., Andersson, J., Tracey, I., 2014. Differential structural and resting state connectivity between insular subdivisions and other pain-related brain regions. Pain 155, 2047–2055. http://dx.doi.org/10.1016/j.pain.2014.07.009.

World Health Organization MONICA Project, 1988. J. Clin. Epidemiol. 41, 105–114. http://dx.doi.org/10.1016/0895-4356(88)90084-4.